Electronic Supplementary Material (ESI) for Green Chemistry.

A Rational Design of Pd-based Catalyst with Metal-Metal Oxide Interface Influencing the Molecular Oxygen in Aerobic Oxidation of Alcohols

Songhita Meher,[a, b] *Rohit K. Rana**[*,a, b]

[a]Nanomaterials Laboratory, CSIR-Indian Institute of Chemical Technology, Hyderabad-500007, India. [b]Academy of Scientific and Innovative Research (AcSIR), Ghaziabad-201002, India.

E-mail: rkrana@iict.res.in.

Experimental Details

Generation of graphene oxide (GO): Graphite oxide was obtained by the oxidation of graphite flake using a modified Hummer method.[1] Typically, 10 g of graphite flake was added in 500 ml of concentrate H_2SO_4 and stirred on ice bath for 1 h. To this, 40 g of $KMnO_4$ was slowly added and the resulted reaction mixture was further stirred for 2 h, after which, the ice bath was removed and stirring was continued for 24 h. The reaction mixture was again put back on ice bath and 500 ml of deionised water was slowly added followed by 30% hydrogen peroxide till the colour of the suspension changed to orange/gold. This was centrifuged at 600 rpm for 10 min to separate the unexfoliated graphite oxide. Then the supernatant solution was centrifuged at a higher speed (4000 rpm) for 30 min to obtain golden coloured solid. Thus obtained solid was dialysed for one week to remove the unwanted salts. Thus prepared GO was re-dispersed in water to get a final concentration of 5 mg/mL for further use.

Synthesis of Pd@rGO: An aqueous suspension of Graphene oxide (40 mL, 1 mg/mL) was sonicated for 30 min and then under the stirring condition, 0.05 mL of hydrazine hydrate (80%) was added drop-wise and stirred for 1 h. Then 470 µl solution of Na_2PdCl_4 (10 mM) was added slowly to the above suspension followed by addition of 500 µl $NaBH_4$ (100 mM). The stirring was continued for 30 min and thus formed black precipitate was centrifuged followed by washing with DI water for five times to obtain Pd@rGO.

Synthesis of PdO@rGO: Graphene oxide (40 mL, 1 mg/mL) was sonicated for 30 min and then under the stirring condition, 0.05 mL of hydrazine hydrate (80%) was added drop-wise and stirred for 1 h. Then 470 µl solution of Na_2PdCl_4 (10 mM) was added slowly to the above suspension followed by addition of NaOH (1.0 M) till the pH of the solution reached 11.0.

The above solution was kept stirring for overnight. The formed black precipitate was centrifuged followed by washing with DI water for five times to obtain PdO@rGO.

Synthesis of Pd Nanoparticles: To an aqueous solution of Na_2PdCl_4 (20 mL, 10 mM) was added 0.05 mL of hydrazine hydrate (80%) slowly followed by heating at 90°C for 12 h. Thus resulted solid was separated via centrifugation followed by washing with DI for 3-4 times to obtain Pd nanoparticles.

Test for heterogeneity of the catalyst: To confirm the heterogeneity of the Pd-PdO@rGO-1.25 catalyst in the oxidation of benzyl alcohol, the catalyst was removed from the reaction mixture after 2 h of the reaction at 353 K and then the reaction was continued without the solid catalyst. It was observed that, the benzyl alcohol conversion did not change after the catalyst was removed. This indicated that the active species are attached with the solid catalyst and there was no leached species in the reaction mixture, which could further catalyze the reaction. So it confirmed the true heterogeneous nature of the catalytic process.

Characterization

Sonochemical process was carried out using Vibra cell (VCX 750, Sonics & Materials, Inc., USA) probe sonicator equipped with titanium alloy tip. Powder X-Ray diffraction (XRD) patterns were recorded on a PANalytical (empyrean, UK) X-Ray Diffractometer using CuKα (λ=1.5406 Å) radiation at 45 kV and 30 mA with a standard monochromator, equipped with a Ni filter to avoid CuKβ interference. The powder XRD patterns were used for identification of the crystalline phases of the precipitated powder and to estimate the crystallite size using the Debye−Scherrer formula [$L=0.9\lambda/(D \cos \theta)$], where λ is the X-ray wavelength, θ is the Bragg angle, and D is the full width at half maximum intensity (FWHM) of the diffraction line (hkl) (converted into radians). HR-TEM and HAADF-STEM with EDS analyses were carried out using Talos F200X TEM. FE-SEM analyses were performed on a JEOL-7610F,

Scanning Electron Microscope operated at 2, 5 and 15kV at working distances of 6, 8 and 15 mm and energy dispersive X-ray spectroscopy (EDX) was performed with an OXFORD Inca detector interfaced at 15 kV without sample sputtering. JEOL Analytical Station software was used for the EDS data analysis. FT-IR spectra were recorded within 400−4000 cm^{-1} on a Bruker ALPHA spectrometer equipped with a DTGS detector. Confocal micro-Raman spectra were recorded on a Horiba Jobin-Yvon LabRam HR spectrometer using a 17 mW internal He−Ne laser source having a wavelength of 632.8 nm. UV−vis absorbance was measured using a Varian Cary 5000 spectrometer. XPS analyses were carried out on a Kratos Analytical AXIS Supra using the Mg Kα anode. The binding energies (±0.1 eV) were determined with respect to the position of the adventitious C 1s peak at 284.8 eV. For elemental analysis, a Perkin Elmer Analyst 300 atomic absorption spectrometer was used. Surface area measurements were done via N2-sorption using a Quanta Chrome gas sorption system (Nova-4000e), and the samples were degassed at 200 °C for 6 h prior to measurement. Dynamic light scattering (DLS) measurements were done with a Zetasizer Nano-ZS (Malvern instruments, UK) using a 173° scattering angle and laser light of wavelength 633 nm.

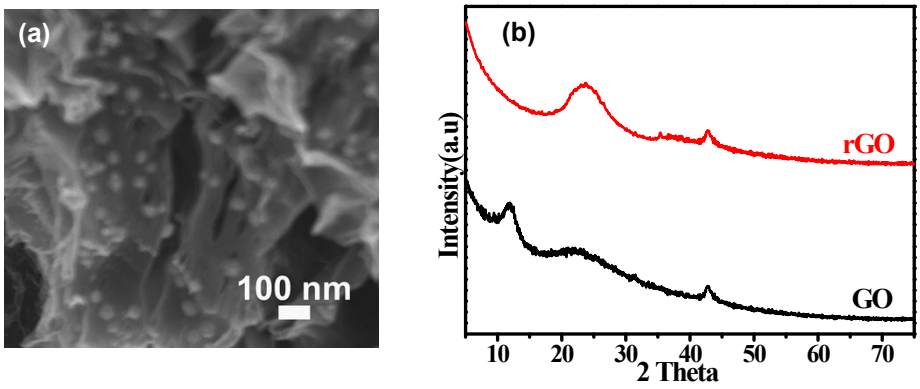

Figure S1. (a) FE-SEM image of the Pd-loaded sample prepared using GO sheets directly without any partial reduction step; (b) XRD patterns of the as-synthesized GO and rGO samples.

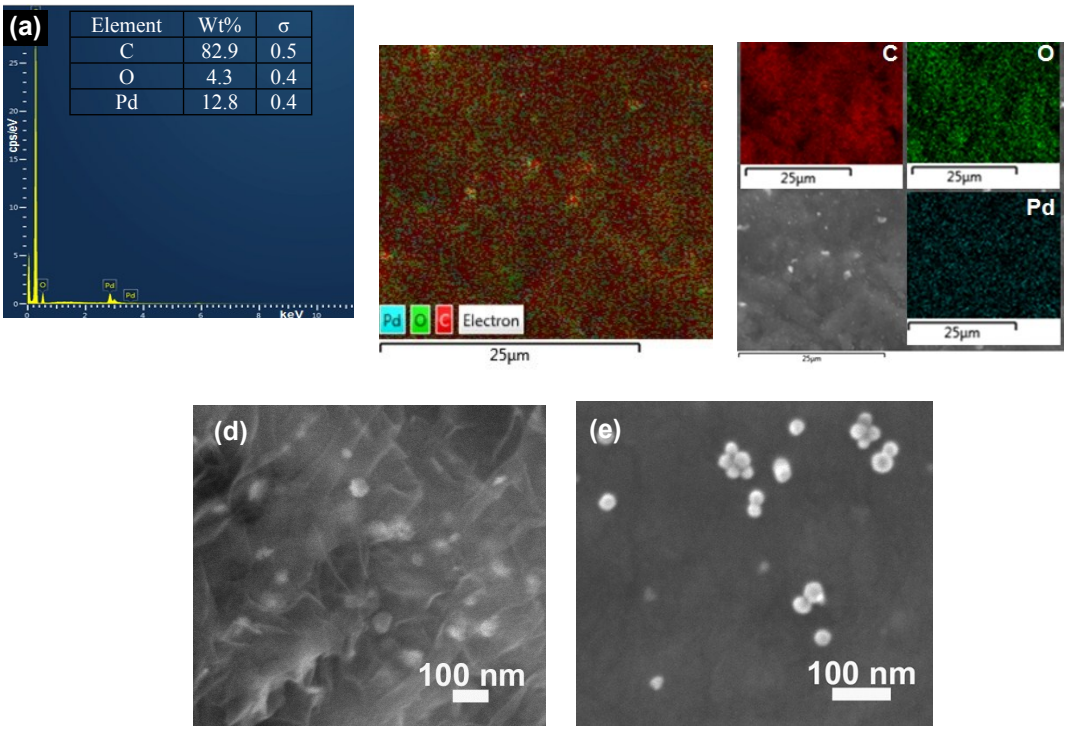

Figure S2. (a-d) EDS analysis of for Pd-PdO@rGO-1.25 showing (a) EDS obtained for the spot analysis on one of the particles present in the FE-SEM image with corresponding elemental composition, (b) elemental mapping with the distribution of different elements, and (c) distribution of individual elements; (d, e) FE-SEM images of Pd-PdO@rGO with 5.0 Wt.% and 2.5 Wt.% of Pd, respectively.

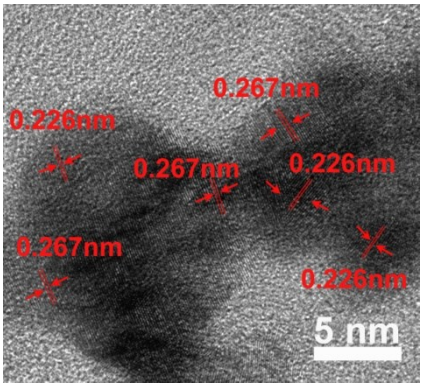

Figure S3. HRTEM image depicting the lattice fringes of Pd and PdO crystallites in Pd-PdO@rGO-1.25.

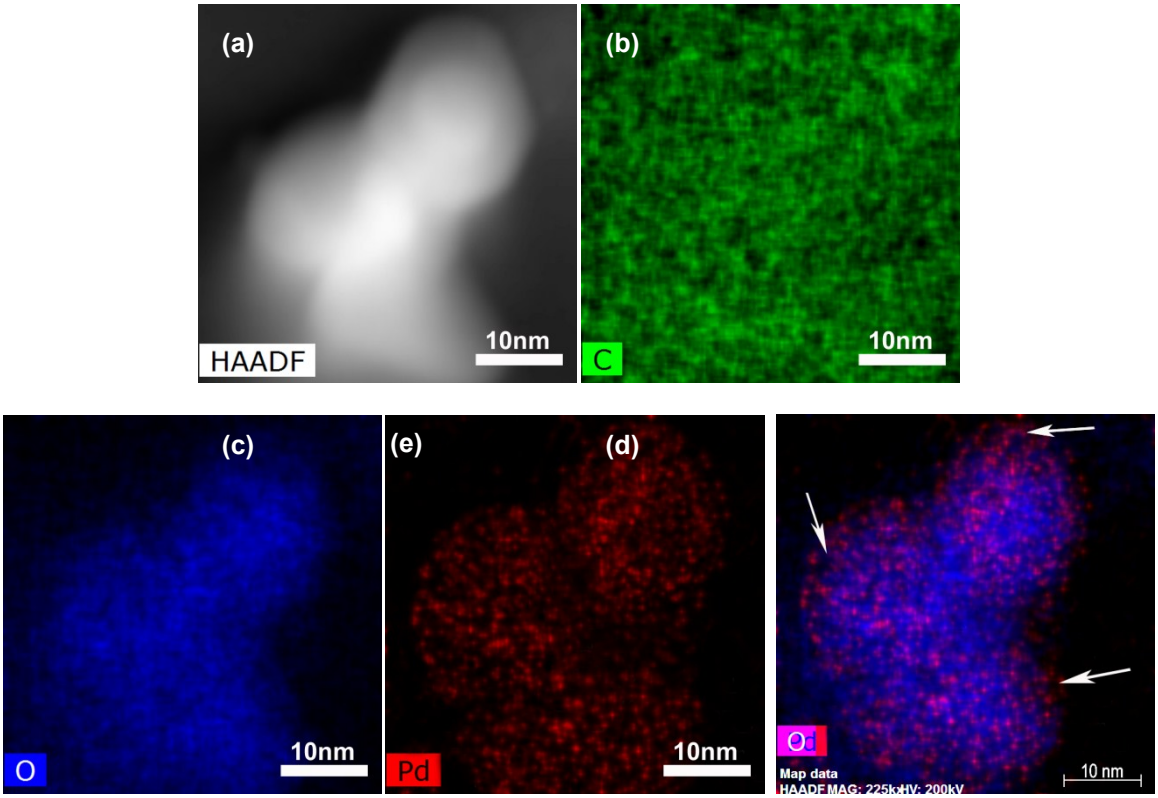

Figure S4. (a) HAADF-STEM image, (b-d) EDS elemental mapping for C, O and Pd, respectively, and (e) the superposed image of Pd and O elements as analysed for Pd-PdO@rGO-1.25. The arrow marks in the image shows the regions wherein the Pd content is dominant compared with that for O element.

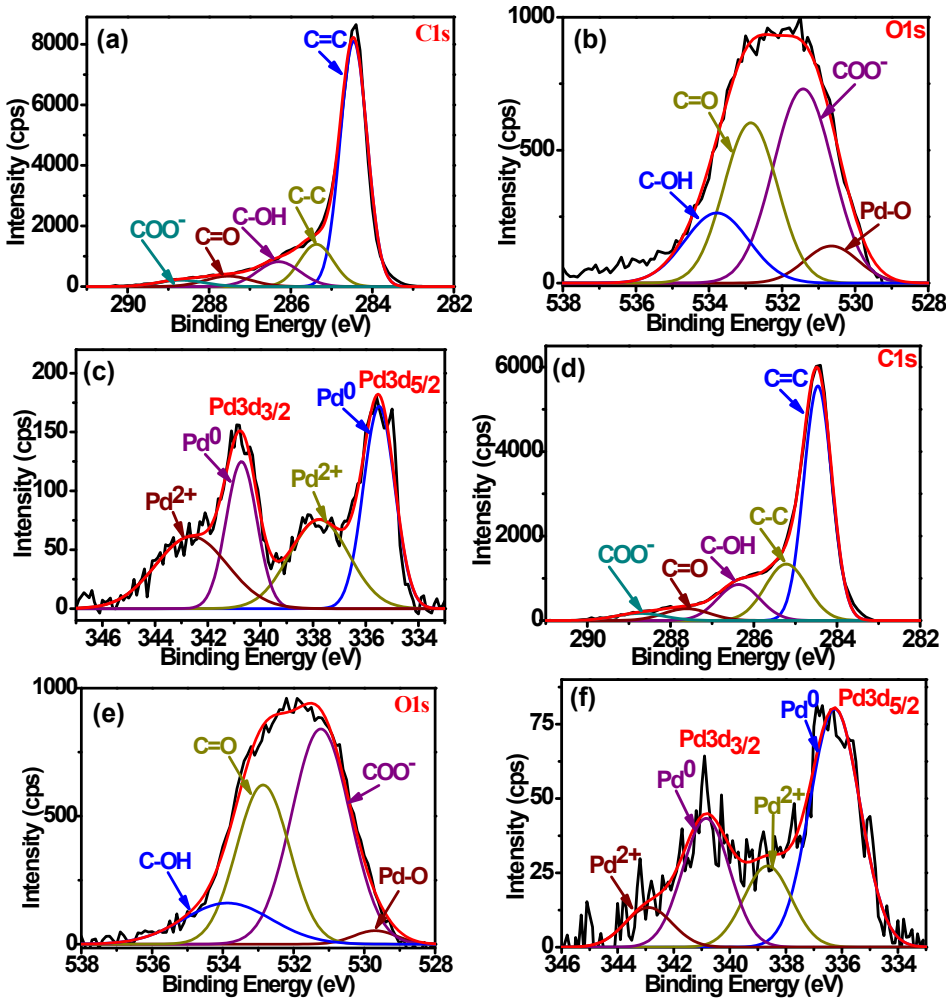

Figure S5. XPS analysis showing (a) C1s, (b) O1s and (d) Pd 3d spectra for Pd-PdO@rGO-5.0 sample; (e) C1s, (f) O1s and (g) Pd 3d spectra for Pd-PdO@rGO-0.625 sample.

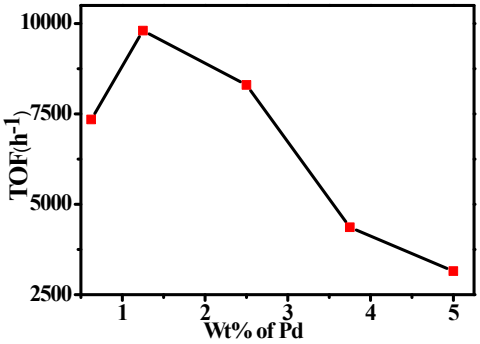

Figure S6. TOF with respect to various Pd-loading in the sample Pd-PdO@rGO-x. Reaction conditions: 20 mg catalyst (Pd-PdO@rGO-1.25), 0.1mol benzyl alcohol, K_2CO_3- 0.3 mol, 5 mL water, O_2 (~1atm), 80 ^oC .

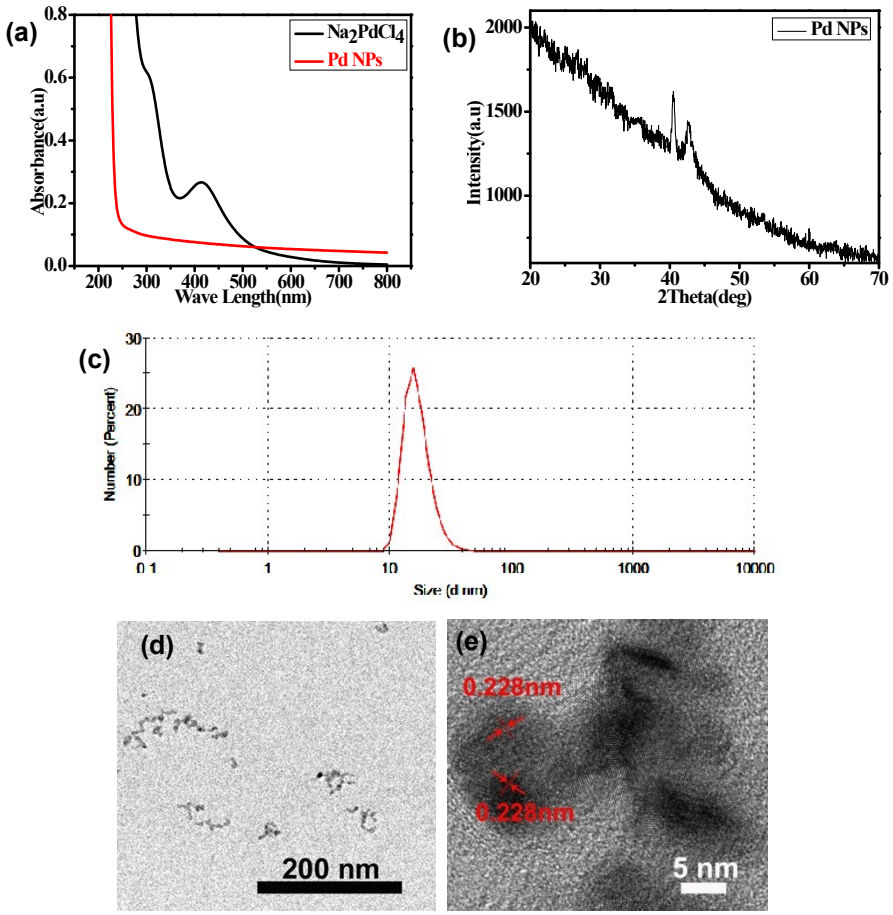

Figure S7. (a) UV-vis spectra of the aqueous solution of Na_2PdCl_4 precursor before and after the reduction process during the synthesis of Pd nanoparticles. The comparison of the UV-vis spectra shows the disappearance of the absorbance due to the precursor after the reduction of Pd^{2+} to form Pd nanoaprticles; (b) XRD, (c) DLS hydrodynamic particle-size distribution, (d) HRTEM image depicting the particle-sizes, and (e) HRTEM image depicting the lattice fringes of the metallic Pd only for the synthesized Pd nanoparticles.

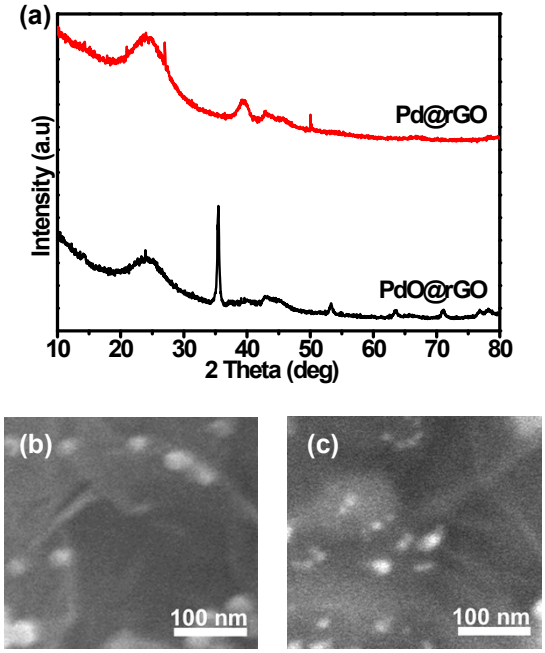

Figure S8. (a) XRD and (b, c) FE-SEM images of PdO@rGO and Pd@rGO samples, respectively.

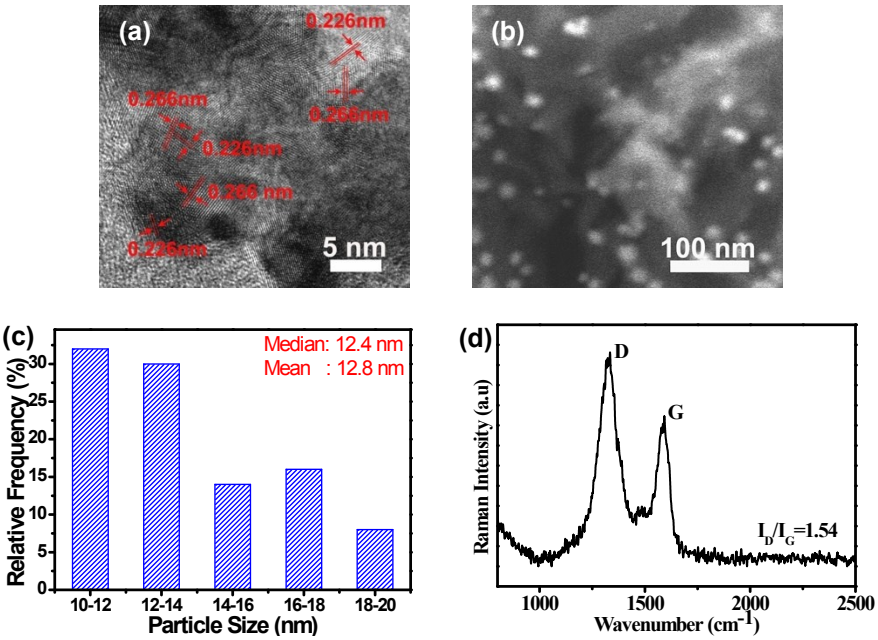

Figure S9. Characterization of the used Pd-PdO@rGO-1.25 catalyst; (a) HRTEM image depicting the lattice fringes for Pd and PdO crystallites; (b) FE-SEM image; (c) particle-size distribution plot (from a count of >50 particles); (d) Confocal micro-Raman spectra.

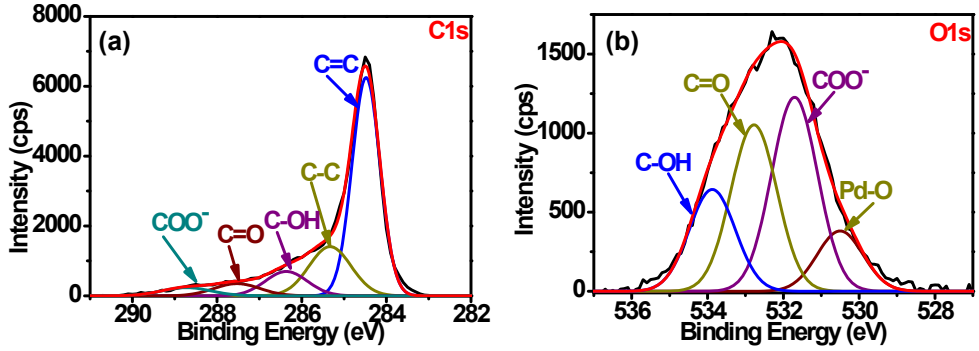

Figure S10. XPS analysis showing (a) C1s, and (b) O1s spectra for the used Pd-PdO@rGO-1.25 catalyst.

Table S1. The Pd-loadings in Pd-PdO@rGO samples as obtained from ICP-OES analysis

Sample	Pd (Wt.%)
Pd-PdO@rGO-0.625	0.625
Pd-PdO@rGO-1.25	1.25
Pd-PdO@rGO-2.5	2.5
Pd-PdO@rGO-3.75	3.75
Pd-PdO@rGO-5	5.0

Table S2. The Crystallite-size determined from XRD and the elemental composition in Pd-PdO@rGO samples as estimated from EDS analysis

Sample	Crystallite Size (nm)[a]		Elemental composition (Wt.%) [b]		
	Pd	PdO	C	O	Pd
Pd-PdO@rGO-0.625	-[c]	-[c]	82.9	16.5	0.6
Pd-PdO@rGO-1.25	2.4	0.54	79.4	19.6	1.0
Pd-PdO@rGO-2.5	-[c]	-[c]	76.0	22.1	1.9
Pd-PdO@rGO-3.75	2.56	0.58	-[c]	-[c]	-[c]
Pd-PdO@rGO-5	2.78	0.65	-[c]	-[c]	-[c]

[a] Determined from XRD using Debye-Scherrer equation, [b] Determined from EDS, [c] Not determined.

Table S3. The PdO:Pd ratio obtained from the XRD and XPS analysis

Sample	PdO/Pd ratio (from XRD)	Pd^{2+}/Pd^{0} ratio (from XPS)
Pd-PdO@rGO-0.625	0.13	0.21
Pd-PdO@rGO-1.25	0.23 0.25 (used)	0.33 0.32 (used)
Pd-PdO@rGO-5	0.38	0.96

Table S4. Optimization of the reaction temperature and solvent in aerobic oxidation of benzyl alcohol using Pd-PdO@rGO-1.25 as the catalyst[a]

Entry	T (°C)	Time (h)	Solvent	Conversion (%)	Selectivity (% of aldehyde)
1	27	24	Water	1.9	43.8
2	60	4	Water	23.4	89.7
3	80	4	Water	92.1	98.26
4	90	4	Water	93	85.3
5	100	4	Water	96.4	82.4
6	80	4	Acetonitrile	61.8	76
7	80	4	Isopropanol	29	68
8	80	4	Toluene	49	79

[a] Reaction conditions: Reaction conditions:20 mg catalyst (Pd-PdO@rGO-1.25), 0.1mol benzyl alcohol, K_2CO_3- 0.3 mol, 5 mL water, O_2 (~1atm).

Table S5. Catalytic activity of various catalysts in the oxidation of benzyl alcohol[a]

Catalyst	Pd-loading (Wt.%)	Conversion (%)	Selectivity (% of aldehyde)	TOF (h^{-1})
No catalyst	-	No	-	-
rGO	-	8	34	**-**
Pd NPs	-	46	22	**622**
Pd/rGO (physically mixed)	1.25	39	40	**4150**
Pd@rGO	1.25	39.1	82	**4274**
PdO@rGO	1.25	21.9	54	**2165**
Pd/C	10.0	81	51	**215.5**

[a] Reaction conditions: Catalyst with 2.35μmol of Pd, 0.1 mol benzyl alcohol, 0.3 mol K_2CO_3, 5 mL water, O_2 (~1atm), 80 °C, 4h. [b] TOF estimated for 1h of the reaction.

Table S6. Effect of histidine addition in the aerobic oxidation of benzyl alcohol using Pd-PdO@rGO-1.25 as the catalyst[a]

Time (min)	Conversion (%)	Selectivity (%)		
		Benzaldehyde	Benzoic Acid	Benzyl benzoate
30	5.0	3.0	-	2.0
60	7.0	4.0	-	3.0
90	8.1	4.45	-	3.65
120	13.3	9.0	-	4.2
240	18.0	12.0	0.45	5.0

[a]Reaction conditions: Reaction conditions:20 mg catalyst (Pd-PdO@rGO-1.25), 0.1mol benzyl alcohol, 0.05 mol histidine, K_2CO_3- 0.3 mol, 5 mL water, O_2 (~1atm).

Table S7. The C:O and PdO:Pd ratio obtained from the XPS analysis of used catalyst

Sample	Oxidized carbon to graphitic carbon ratio (C1S)	C1S/O1S ratio	Pd^{2+}/Pd^0 ratio
Pd-PdO@rGO-1.25 (used)	0.93	2.96	0.32

Table S8. Summary of various Pd-based heterogeneous catalysts reported for the aerobic oxidation of benzyl alcohol

Catalyst	**Pd-Loading (Wt.%)**	**Particle size(nm)**	**Pd oxidation states (The one in bold is attributed for the catalytic activity)**	**Condition**	**Conv. (%)**	**Select. (Ald.) (%)**	**TOF (h^{-1})**	**Remarks**	**Ref**
Pd-PdO@rGO	1.25	10-20	**Pd^0,** **Pd^{2+}** (PdO)	H_2O/80˚C/O_2 (~1 atm.)/4h	92.1	98.26	9801 (18000 at 1h)	Efficient with respect to conv., select. & TOF together	**This work**
Pd on Graphene	0.68	4.1	**Pd^0**	Solvent free/110˚C/O_2(20 ml/min)/ 6 h.	72.5	96	30,137	Low conv.	**2**
Pd-GO-P123	1.7	40	No XPS data **Pd^0**	(Surfactant/H_2O) /80 ˚C/O_2(1 atm), 3.5h	-	98% yield	175.14	Low TOF	**3**
Pd/COP	1	7.7 ± 1.8	No XPS data **Pd^0**	Solvent free//160˚C/O_2(30 ml/min)/ 8 h.	32.0	57.1	95 411	High temp.; Low conv. & select.; TOF is for 1st 15 min	**4**
Pd/APS-S16	2	2.8	No XPS data **Pd^0**	solvent free /140˚C/ O_2(20ml/min)/ 1 h.	21.0	94.6	7858	low conv.	**5**
Pd on Fe doped SBA-15	3	3	No XPS data **Pd^0**	Solvent free/85˚C/O_2 bubbling at atm pr/9 h.	71	83.2	633	Low conv. & TOF	**6**
Pd/SiO_2-Al_2O_3	0.52	3.1	**Pd^0**	Solvent free /70˚C/ O_2(3 $mLmin^{-1}$)/ 10 h.	68	98	8820	Low conv.	**7**
Pd/MIL-101	0.35	3	**Pd^0**	Toluene/160°C/ O_2 (20 mL min^{-1})/ 1.5 h.	99	99	16 900 (1h)	Higher temp	**8**
Pd HAP-0		4-5 nm	**Pd^0**	Water/110°C/O_2 atm/1 h.	99	89	9800	Higher temp.	**9**
Pd/rGO-E-100	1.4	0.9	**Pd^{2+}**	H_2O/(0.5MPa)O_2/ 1h./ 60°C 80 ˚C	98.9 90.3	99.9 95.8	1960 12047	Higher O_2 pressure	10
Pd NPs/PS	-	30-40nm	**Pd^0**	Air/Toluene/85 ˚C/K_2CO_3/15 h.		Yield-99	-	Toluene solvent; More Pd is used (low TOF); longer reaction time	**11**
Pd@hmC	-	5nm	**Pd^0**	H_2O/80˚C/O_2(1 atm)/ 1 h.	48	37	2940	Low conv., select. & TOF	**12**

Pd/NaX	1.35	2.8	**Pd^0**	Solvent free/100˚C/O_2,3 mL min/4 h.	66	97	626	Low TOF	**13**
0.5%Pd@C-GluA-550	0.5	5.9	**Pd^0** and Pd^{2+}	Solvent free/20 mg /120˚C/air 1 atm/34 h. Solvent Free/10 mg /120˚C/O_2 0.1 MPa/0.5 h.	48.8 --	63 76	14802 15355 1 (0.5h)	Higher temp.; long reaction time; Low conv. & select.	**14**
Pd/meso-Al_2O_3	0.06	0.8	**Pd^{2+}**	Toluene/60˚C/air/ 24 h.		99	4096 (1 h)	Low conv., select. & TON; Longer reaction time	**15**
Pd/Al_2O_3–N **Pd/Al_2O_3–H**	2.56 2.68	6.5 7.2	**Pd^0** and Pd^{2+}	120˚/ O_2 50 mL/min/ 8 h 100˚/ O_2 50 mL/min/ 8 h	80.1 63.5	94.3 96.5	3615 2865	Low conv. & TOF	**16**
1%Pd/TiO_2 - 0.005APTES	0.96	3.4	**Pd^0**, Pd^{2+} and Pd^{4+}	Solvent Free/120˚ C/O_2-1 bar/7 h	61.5	81.4	Yield 42.7	Low conv. & select.	**17**
Pd@U-E15 (BFPMO)	0.086 mmol/g		Pd^{2+} ; **Pd^0 -** found in the used catalyst	H_2O/90°C/1 atm of O_2/ K_2CO_3/15 h	90	90	12	Low TOF& Longer reaction time	**18**
Pd/CeO_2	0.074 wt%	Atomically dispersed	**Pd^0** ; Pd-O linkage (Pd oxidation state <2)	100°C/1 atm O_2/3 h.		>99	6739	Low TOF	**19**
BT15−Pd NPs	Aqueous Colloid	3.23	**Pd^0**	H_2O/50°C/ 1 atm O_2/ K_2CO_3/24 h.	99.89	--	2.081	Low TOF; Catalyst as a colloid; Longer reaction time	**20**

References:

1. J. Y. Kim, W. H. Lee, J. W. Suk, J. R. Potts, H. Chou, I. N. Kholmanov, R. D. Piner, J. Lee, D. Akinwande and R. S. Ruoff, *Adv. Mater.,* 2013, **25**, 2308–2313.

2. G. Wu, X. Wang, N. Guan and L. Li, *Appl. Catal. B.,* 2013, **136–137***,* 177–185.

3. S. Rostamnia, E. Doustkhah, Z. Karimi, S. Amini and R. Luque, *ChemCatChem*., 2015, **7**, 1678 – 1683.

4. Y. Zhou, Z. Xiang, D. Cao and C. J. Liu, *Ind. Eng. Chem. Res.,* 2014, **53**, 1359−1367.

5. Y. Chen, H. Lim, Q. Tang, Y. Gao, T. Sun, Q. Yan and Y. Yang, *Appl. Catal. A.,* 2010, **380**, 55–65.

6. Y. Li, J. Huang, X. Hu, L. Y. LamFrank, W. Wang and R. Luque, *J. Mol. Catal. A.,* 2016, **425**, 61-67.

7. J. Chen, Q. Zhang, Y. Wang and H. Wan, *Adv. Synth. Catal.,* 2008, **350**, 453 – 464.

8. G. Chen, S. Wu, H. Liu, H. Jiang and Y. Li, *Green Chem.,* 2013, **15**, 230–235.

9) K. Mori, T. Hara, T. Mizugaki, K. Ebitani and K. Kaneda, *J. Am. Chem. Soc.,* 2004, **126**, 10657–10666.

10. L. Lei, Z. Wu, R. Wang, Z. Qin, C. Chen, Y. Liu, G. Wang, W. Fan and J. Wang, *Catal. Sci. Technol.,* 2017, **7**, 5650–5661.

11. K. Karami, M. Ghasem and N. N. Haghighat, *Catal. Commun*., 2013, **38**, 10–15.

12. T. Harada, S. Ikeda, F. Hashimoto, T. Sakata, K. Ikeue, T. Torimoto and M. Matsumura, *Langmuir,* 2010, **26(22)**, 17720–17725.

13. F. Li, Q. Zhang and Y. Wang, *Appl. Catal. A.,* 2008, **334**, 217–226

14. P. Zhang, Y. Gong, H. Li, Z. Chen and Y. Wang, *Nat. Commun.,* 2013, ***4***, 1593–1-11.

15. S. F. J. Hackett, R. M.Brydson, M. H. Gass, I. Harvey, A. D. Newman, K. Wilson and A. F. Lee, *Angew. Chem. Int. Ed.,* 2007**, 46***,* 8593–8596.

16. X. Wang, G. Wu, N. Guan and L. Li, *Appl. Catal. B.,* 2012, **115***, 7– 15.*

17. P. Weerachawanasak, G. J. Hutchings, J. K. Edwards, S. A. Kondrat, P. J. Miedziak, P. Prasertham and J. Panprano, *Catal. Today,* 2015, **250**, 218-225.

18) B. Karimi, M. Khorasani, H. Vali, C. Vargas and R. Luque, *ACS Catal.,* 2015, **5**, 4189−4200.

(19) P. Xin, J. Li, Y. Xiong, X. Wu, J. Dong, W. Chen, Y. Wang, L. Gu, J. Luo, H. Rong, C. Chen, Q. Peng, D. Wang and Y. Li, *Angew. Chem. Int. Ed.,* 2018, **57**, 4642–4646.

(20) B. Hao, M. Xiao, Y. Wang, H. Shang, J. L. Ma and M. H. Yang, *ACS Appl. Mater. Interfaces*, 2018, **10**, 34332−34339.